https://doi.org/10.5194/egusphere-2026-2457
Preprint. Discussion started: 15 July 2026

Spatial Modelling of Ice-Jam Susceptibility in Southern Quebec: An Enhanced Ice Jam Predisposition Index

Elnaz Mirzaei[1,2,3], Karem Chokmani[1,2,3], Rachid Lhissou[4], Saeid Homayouni[1,2,3]

[1]Centre Eau Terre Environnement, Institut National de la Recherche Scientifique (INRS), Québec, QC, Canada
[2]Centre d'études nordiques (CEN), Université Laval, Québec, QC, Canada
[3]Réseau Inondations Intersectoriel du Québec (RIISQ), Montréal, Canada
[4]Canada Water Agency, Environment and Climate Change Canada, Québec, Canada

Correspondence to: Elnaz Mirzaei (Elnaz.mirzaei@inrs.ca)

Abstract: Ice jams represent a recurrent natural hazard in Quebec, where geomorphological and structural river characteristics play a key role in determining their spatial distribution. This study improves and evaluates the Ice Jam Predisposition Index (*IJPI*) using a dataset of 35 rivers across southern Quebec. The enhanced model integrates geomorphological parameters, including channel narrowing, sinuosity, and slope, along with structural (bridge) and hydrological (tributary) features to delineate reaches prone to ice-jam formation. Including rapids as an inverse indicator helps distinguish high-energy segments where jams are unlikely to occur. Model validation shows that over 90 % of observed ice jams occurred in reaches with medium to high predisposition, with an overall recall of 0.90, indicating promising performance as a screening tool. The results highlight the dominant influence of flat slopes, channel confinement, and curvature on jam formation, suggesting that the model can serve as a useful spatial tool for regional ice-jam risk management. These results demonstrate the potential of the proposed framework to support operational flood risk management by allowing proactive identification of vulnerable river sections. Decision-makers and emergency management agencies can use the model to prioritise monitoring efforts and improve preparation for ice-jam-related hazards.

Keywords: ice jam, river geomorphology, spatial flood risk mapping, cold-region hydrology

1 Introduction

Over one-third of Earth's landmass is drained by rivers that experience seasonal freezing. Ice can markedly alter the hydrologic, ecologic, climatic, and socio-economic functions of these river corridors (Yang et al., 2020). The annual cycle of river ice formation, growth, decay, and clearance includes several phenomena, including low flows, ice jams, and mid-winter and spring break-up events (De Rham et al., 2020). An ice jam develops when the flow of ice floes is blocked along a section of a river. It could occur due to factors such as existing ice blocks, variations in river slope, meandering channels, man-made structures such as bridges, and natural structures such as islands. This obstruction causes incoming ice to accumulate upstream, thereby creating a pack that gradually extends in length, and which contributes substantially to the severity of flooding (Beltaos, 1995).

https://doi.org/10.5194/egusphere-2026-2457
Preprint. Discussion started: 15 July 2026

Subsequent flood damage tends to be extensive. In fact, the resulting floods can be both socio-economically costly and life-threatening (Beltaos, 1997). The U.S. Army Corps of Engineers (2004) estimates that ice jam damages in the United States alone exceed 100 million USD annually (Morgan et al., 2004). Several significant ice-jam events have likewise been documented in Canada, including the 2020 Fort McMurray event (Northern Alberta), which caused over 500 million CAD in damage and displaced 13,000 people (The Insurance Bureau of Canada, 2025). The financial costs of ice jam floods (IJFs) are challenging to estimate, but a comprehensive economic assessment of the damage has yet to be conducted (Beltaos and Prowse, 2009). It has been estimated that the annual cost for North America is 300 million USD, based upon 2017 cost estimates and adjusted for historical inflation (French, 2018). Given the significant risks posed by flooding, it is essential to identify vulnerable areas, assess potential impacts, and develop appropriate mitigation strategies. To aid this process, government agencies, emergency managers and insurers must rely upon clear, reliable tools to estimate expected damage to existing and future structures and infrastructure in flood-prone regions (Oubennaceur et al., 2019).

IJFs tend to occur much more rapidly than open-water floods, with water levels frequently rising by more than a metre in less than an hour (She et al., 2009). What makes IJFs particularly dangerous is their unpredictability (Rokaya et al., 2018). These floods often occur suddenly and are difficult to anticipate, leaving little time to implement contingency measures, especially evacuation (Mahabir et al., 2006; Massie et al., 2002). Yet, estimating and understanding ice jams is important for implementing early warning systems. These systems grant valuable time to respond to and minimise short-term damage, while also helping communities prepare for long-term risks. Accurately forecasting the timing of ice break-up is essential to support emergency responses to river ice-related flooding (Sun, 2018).

Despite extensive research and development focused on forecasting open-water flooding (Beven et al., 1984; Campolo et al., 1999; Cloke and Pappenberger, 2009), limited progress has been made in predicting floods associated with river ice break-up. Forecasting authorities rely heavily upon experience and knowledge of break-up and ice jams within a watershed, together with real-time observations of ice conditions and river gauge data (Beltaos et al., 2012). Given the severity of flooding and the rapid onset of such events, having an accurate and reliable forecasting model would be highly beneficial for informing flood preparedness efforts.

Prior to the introduction of AI and soft computing, traditional prediction methods primarily relied on empirical techniques, statistical analyses, and fluid-dynamic models (White, 1996). Even though effective in particular contexts, these approaches have considerable limitations, especially in precisely capturing the chaotic and localised nature of ice jams (White, 2003). As ice jams are highly dependent on local river morphology and environmental conditions, these models have often lacked generalizability and have not been easily transferable across locations (Mahabir et al., 2007). More recently, data-driven approaches that are based on hydroclimatic variables, including artificial neural networks and fuzzy-logic models, have been explored as credible alternatives for ice-jam forecasting (Madaeni et al., 2020).

In addition to predictive methods, research on ice jams focuses on various aspects, including mapping vulnerable areas and assessing ice maturity. Geomorphological mapping techniques analyse river features, providing important insights into the geospatial characteristics of river systems, upon which the predictability of ice-jam formation and associated flood risk heavily depends. Channel morphology plays a vital role in the occurrence and formation of ice jams along rivers (Lindenschmidt and Das, 2015). Locations that are prone to ice jamming are often associated with specific river geometries, such as bends, slope reductions, and natural (e.g., islands) or artificial (e.g., bridges) flow constrictions (Beltaos, 2008b). Various studies have been carried out to determine the relative importance of different geometric parameters in triggering ice jam formation.

Empirical and modelling studies have consistently stressed the influence of these factors. For example, Buzin (2004) highlighted high water levels during freezing, repeated ice movements, and abundant upstream ice as major contributors, and emphasised that features such as narrow channels, bends, islands, and tributaries create favourable conditions for ice jam formation. Investigations across Russian basins and Canadian rivers have shown that such morphological elements strongly correlate with the frequency and location of ice jams, with narrowing present in up to 90 % of annual events and bends or islands often acting as primary triggers (Kalinin, 2008; Kozlov and Kuleshov, 2019). Studies on the hydraulic interaction between ice and bridge structures have also shown that bridge piers can restrict ice flow, thereby increasing local flood risks (Beltaos et al., 2006). In parallel, several modelling studies have sought to calculate these influences. Physical flume experiments and 3D computer simulations have shown that channel-width restrictions, along with slope and depth variations, play a primary role in initiating jams (Taha et al., 2022). Machine learning and geospatial approaches, including decision tree and clustering algorithms, have successfully mapped high-risk zones through integrating geomorphological parameters, achieving high predictive accuracies in some cases (Kowshal et al., 2021).

To methodically evaluate where rivers are most prone to ice jams, researchers have developed composite indices that integrate multiple geomorphological characteristics into a single spatial framework. One of the most comprehensive of these is the Ice Jam Predisposition Index (*IJPI*), which was introduced by De Munck et al. (2017). By applying weighted indices of key morphological features, such as channel constrictions, bends, shallow sections and areas of reduced slope, the *IJPI* captures how these factors merge to influence ice jam formation. Their study demonstrated that ice runs are particularly likely to trigger jams when encountering narrow, meandering, or gently sloped river segments, establishing a clear geographical correlation between river geometry and historical ice-jam events. As a result, the *IJPI* provides an effective tool for pinpointing river sections with a higher predisposition to ice jams, delivering valuable insights for managing and mitigating ice-related flood risks (De Munck et al., 2017).

Despite progress in both predictive and geomorphological approaches to ice-jam analysis, several limitations remain in identifying jam-prone river reaches at regional scales. Present methods are often either site-specific, relying upon detailed hydraulic modelling that is not easily transferable, or fail to consistently integrate multiple geomorphological controls inside a unified, operational framework. In particular, the influence of certain structural and hydraulic features, such as bridges, tributaries and rapids, is not always explicitly incorporated or systematically evaluated across large river networks.

To address these limitations, this study intends to refine and extend the Ice Jam Predisposition Index (*IJPI*) within a GIS-based framework through analysing 35 rivers in southern Quebec (Canada). The proposed approach assimilates key geomorphological parameters, including channel narrowing, sinuosity, and slope, while clearly accounting for the effects of

https://doi.org/10.5194/egusphere-2026-2457
Preprint. Discussion started: 15 July 2026

bridges, tributaries and rapids. In particular, the inclusion of rapids as an additional geomorphological indicator extends the original *IJPI* formulation.

The objective of this study is therefore to provide a consistent and transferable system for identifying ice-jam-prone reaches at the regional scale, to support flood-risk management and improve preparedness in cold-region river systems.

2 Methodology

2.1 Conceptual framework for assessing ice jam predisposition

The occurrence of ice jams in riverine systems is a complex phenomenon resulting from the interplay between hydrometeorological drivers, such as freeze-up and break-up flows, ice thickness and temperature fluctuations, and geomorphological constraints that are imposed by the river channel. Extensive studies (Beltaos, 2008a; Das et al., 2017) have demonstrated that while climatic forcing initiates ice movement, the spatial localisation of ice jam formation is primarily governed by channel morphology. Constrictions, bends, and slope transitions reduce ice transport capacity, promote ice floe accumulation, and increase the likelihood of arrest and arching (Beltaos, 2013).

More broadly, ice-jam risk is not solely determined by channel morphology but is influenced by ice-cover conditions, hydrometeorological triggers, and channel predisposition. This integrated perspective has been operationalised in systems such as the DAVE framework, where these three components jointly determine the likelihood of ice-jam occurrence (Chokmani et al., 2022).

Building on this understanding, De Munck et al. (2017) proposed a multi-parametric index, the Ice Jam Predisposition Index (*IJPI*), to quantitatively assess spatial predisposition to ice jam formation. This index integrates key geomorphological parameters known to affect ice transport dynamics: channel narrowing, sinuosity, slope breaks, and the modifying presence of islands, bridges, and tributary confluences. In the present study, this framework is adopted and enhanced by incorporating rapids as hydraulic controls that modify local predisposition by disrupting ice arch stability in predictable ways.

Operationally, the implemented *IJPI* uses three geomorphological predictors measured per reach: channel narrowing (*NI*), sinuosity (*SI*), and slope, while bridges and tributary confluences are represented as width adjustments upstream of *NI* detection. Islands are not explicitly parameterised in the current implementation; their influence is captured implicitly through platform-width measurements. Classification of *NI*, *SI*, and slope relies on fixed thresholds that are held common across rivers (rather than unsupervised clustering), and aggregation uses fixed weights, followed by deterministic hydraulic post-rules (neighbour boost, masking rapids) to encode local context.

https://doi.org/10.5194/egusphere-2026-2457
Preprint. Discussion started: 15 July 2026

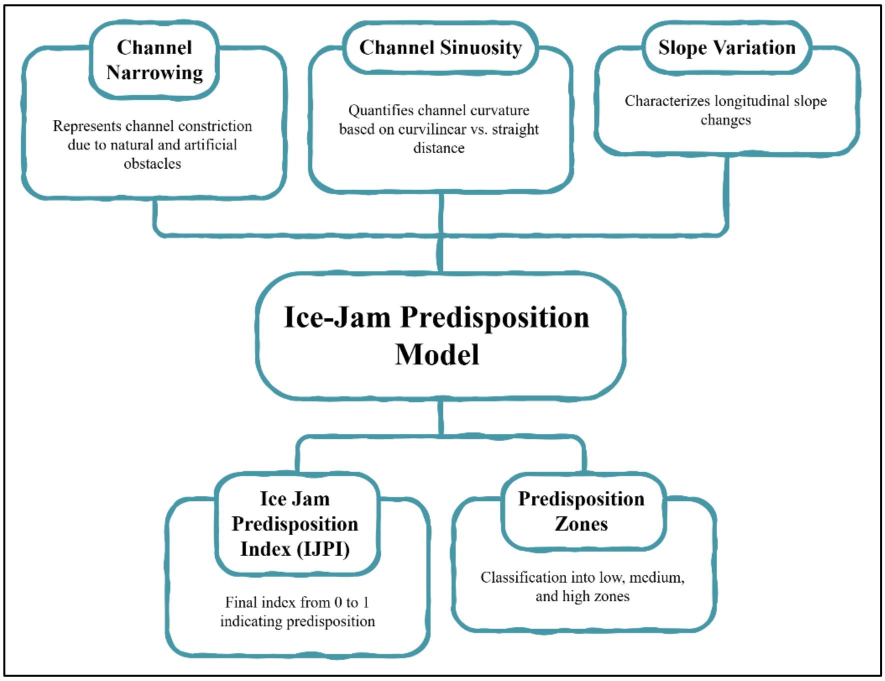

Figure 1: Conceptual framework of the ice-jam predisposition model (adapted from De Munck et al., 2017), illustrating the geomorphological factors that are used to derive the Ice Jam Predisposition Index (*IJPI*) and classify river reaches according to their susceptibility to ice-jam formation.

2.2 Study area selection and river selection

A total of 35 rivers across southern Quebec were selected for analysis. Among these, 12 rivers are particularly vulnerable, having experienced frequent and severe ice jams, while the remaining rivers have recorded more than one ice jam event. These rivers were selected based on documented historical ice-jam events recorded in the provincial ice-jam database maintained by the Ministère de la Sécurité publique du Québec (MSP) (MSP, 2024). The selection was also corroborated through expert consultations. This region is characterised by a humid continental climate with prolonged freeze-thaw cycles, which is particularly prone to ice jams due to frequent mid-winter thaws and high spring freshets (Lindenschmidt and Das, 2015).

https://doi.org/10.5194/egusphere-2026-2457
Preprint. Discussion started: 15 July 2026

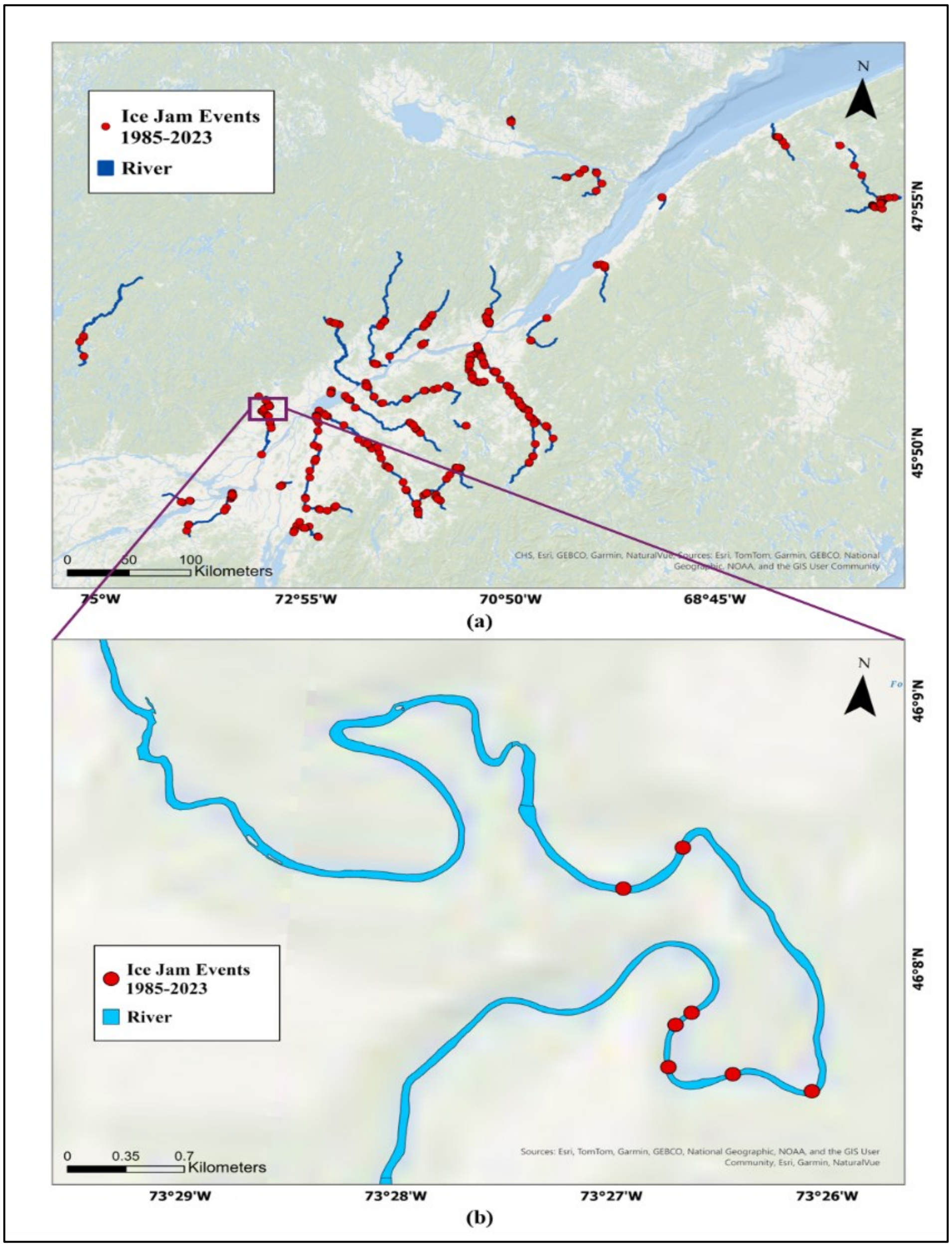

Figure 2. The study area in southern Quebec is centred on the St. Lawrence River valley and indicates rivers that have historically been affected by ice jams. (a) Regional overview of the study area with the spatial distribution of documented ice-jam events (1985–2023) across southern Quebec. (b) Detailed example of a representative reach of the L'Assomption River, illustrating the alignment of recorded ice-jam locations along the channel network. Map created by the authors using ArcGIS from historical ice-jam records and geospatial datasets compiled for this study. Sources: Esri, TomTom, FAO, USGS | Powered by Esri.

2.3 Input Data and River Segmentation

To characterize river morphology, a set of publicly available geospatial datasets was assembled from official provincial data sources. River polygons and hydrographic features were obtained from the Géobase du réseau hydrographique du Québec (GRHQ), distributed through Données Québec. The shapefile download index used for data acquisition corresponded to the 2024 version available at the time of data compilation (MRNF, 2024). River centrelines, islands, and tributary features used in the analysis were derived from this primary hydrographic dataset. The extracted centrelines were checked for connectivity and topological consistency and converted into single-part polylines to facilitate subsequent segmentation and index calculation. Island and tributary features were also manually verified and corrected where partially submerged, disconnected, or morphologically complex features were present.

Bridge locations were extracted from the public "Structure" dataset distributed through Données Québec by the Ministère des Transports et de la Mobilité durable du Québec (MTMD), using the version available at the time of data compilation in 2024 (MTMD, 2024). Only structures corresponding to bridges or intersecting the river network were retained for the analysis. LiDAR-derived digital terrain models (DTMs; modèles numériques de terrain, MNTs) were obtained from provincial terrain datasets distributed through Données Québec and used for fine-scale slope computation and for detecting abrupt gradient changes along the river profile (MRNF, 2024). Finally, high-resolution imagery from Google Earth and Bing Maps, consulted during data compilation in 2024, was used to manually delineate and verify rapids and other hydraulic features where automated extraction was not feasible.

Each river centreline was segmented into 250 m reaches in ArcGIS Pro (ESRI, Redlands, CA). The segmentation distance was selected to effectively capture local morphological variability, including features such as alternating pools and riffles, constrictions and bends, while maintaining a sufficiently high number of discrete reaches to allow for robust spatial analysis across each river's course. Short measurement intervals tend to overestimate channel constriction while underestimating sinuosity. Conversely, longer intervals often underrepresent narrowing and fail to capture the influence of minor features such as islands and bridges (De Munck et al., 2017). After segmentation, upstream-to-downstream ordering was enforced so that reaches are indexed with Id = 1, 2, …, N without gaps. This ordering is required by the narrowing algorithm and by the post-classification neighbour rapid rules (De Munck et al., 2017).

2.4 Derivation of Geomorphological Parameters

2.4.1 Narrowing Index (NI)

Channel narrowing is a primary driver of ice jam formation. According to Beltaos (2008a), when ice flows encounter a reach narrower than the critical transport width for the prevailing discharge and ice thickness, the flow becomes insufficient to carry ice floes downstream, leading to accumulation and eventual arching. Kalinin (2008) likewise showed that more than 90 % of ice jams in Russian catchments occurred at sites of abrupt narrowing. This relationship is reinforced by Lindenschmidt and Das (2015), who demonstrated that constricted reaches along the Slave River (Northwest Territories, Canada) accelerate break-

https://doi.org/10.5194/egusphere-2026-2457
Preprint. Discussion started: 15 July 2026

up onset by concentrating flow energy, whereas wider sections persistently retain ice. Their findings show that local reductions in channel width fundamentally govern ice cover stability, fragmentation, and the spatial propensity for ice-jam formation.

Given that ice jam formation is rarely governed solely by channel narrowing but rather arises from the interplay of multiple morphological controls, our model integrates and weights several contributing factors to capture this complexity. In addition to natural variations in channel width, we explicitly incorporate the constricting effects of bridges, the flow disruptions that are caused by islands, and the reduction in effective channel capacity at tributary confluences, all of which have been shown to affect local ice stability and accumulation significantly (Benda et al., 2011; Lindenschmidt et al., 2012; De Munck et al., 2017). Field observations reported by Kalinin (2008) support this approach, showing that 50 % of ice jams occurred at river bends and 46.9 % at channel narrowing points. Islands, bridges, and tributary confluences were associated with 31.3 %, 25 %, and 15.6 % of cases, respectively, thereby emphasising the need to account for these geomorphological features in predictive modelling. Each of these features influences ice jam formation in its own way, by redirecting flow that reduces the river's capacity to carry ice, or by creating spots where ice can easily build up. Nevertheless, for the sake of simplifying the model, we treat all of them as factors that effectively reduce the available space for ice to move through the channel.

Typically, islands cause a constriction in the main river channel (Beltaos et al., 2006) and introduce a transition in slope from steep to gentle. This change compels the moving ice to decelerate and can obstruct the channel flow. Conceptually, such zones are prone to ice jamming; however, in the current implementation, islands are not parameterised as separate predictors. Their influence is captured only to the extent that they alter the measured platform width used in the narrowing analysis. It should be further noted that the potential alleviation of pressure due to partial diversion of ice and water into a secondary channel is not represented.

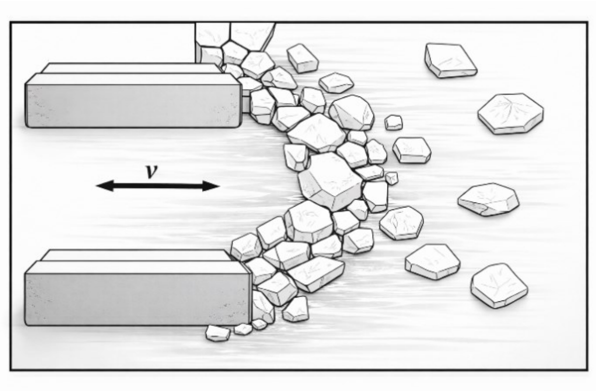

Figure 3: Schematic representation of arch-shaped ice floe accumulation upstream of bridge piers (adapted from (Kawai et al., 1997)).

Bridges, too, required simplification. Bridges can obstruct the movement of river ice and promote the development of ice jams (Kalinin, 2008). In fact, as ice floes approach bridge pillars, certain conditions, such as low flow velocity, may trigger the formation of arch-like ice congestion upstream of the pillars. This phenomenon can occur during both the river's freeze-up

https://doi.org/10.5194/egusphere-2026-2457
Preprint. Discussion started: 15 July 2026

and break-up periods. Figure 3 illustrates a conceptual representation of this arch-shaped ice congestion forming in front of bridge piers.

In addition to triggering arch-like ice congestion, bridge piers act as hydraulic bottlenecks, especially under ice-water two-phase flow conditions. When floating ice exceeds the transport capacity of the narrowed cross-section, particularly between pier columns, ice accumulates at the surface, leading to partial or full blockages. This accumulation can escalate into ice jams, leading to canal bank overflows or breaches. In artificial channels, such pier-constricted sections have been shown to obstruct ice movement more than bends or meanders (Mu et al., 2020). Beyond the mere presence of bridge piers, their position within the cross-section has been shown to substantially influence ice transport and the likelihood of jam formation. Disturbances are particularly pronounced when piers are closely spaced or near the channel centreline (Urroz et al., 1994). The geometry of bridge piers also plays a crucial role in modulating ice accumulation, as certain shapes promote smoother ice passage and reduce the likelihood of blockage (Tymiński, 2010).

Bridges, therefore, function as both obstacles and constraints. Hydraulically, piers subdivide the main channel into narrower sub-channels, thereby increasing the likelihood of jams. In the operational model, the presence of a bridge is represented by a uniform 50 % reduction in channel width within intersected reaches (reflecting limited metadata on pier number/spacing/shape); this parameter may be adjusted when site-specific information is available, and bridges posing negligible risk may be excluded from the inputs.

The tributary represents the final parameter requiring generalisation. Tributaries can introduce additional discharge and fragmented ice at confluences, intensifying the likelihood of severe jams during spring break-up (Kowshal et al., 2021). Break-up in smaller streams often initiates earlier than in the main stem due to steeper gradients and faster runoff response, potentially dictating the break-up sequence and producing multiple jams downstream of confluences (Blouin et al., 2021). Sediment that is supplied by tributaries may further obstruct transport near confluences. Conceptually, a tributary is treated as an effective constriction of the main channel, and susceptibility is inferred through a reduction in local conveyance width proportional to tributary size. In this study, the adjustment is based on the mean tributary width at the confluence, which provides a generalised but consistent representation of tributary influence on narrowing detection.

To quantify these effects, a modified channel width $W_{modified,i}$ was assigned to each reach i. Let $W_{original,i}$ denote the mean measured width of the main channel, $W_{trib,i}$ the mean tributary width intersecting the reach, and B_i a binary bridge indicator equal to 1 when a bridge is present and 0 otherwise. In the operational implementation, width correction was applied according to the dominant local constraint that is represented in the reach attributes:

$$W_{modified,i} = \begin{cases} W_{original,i} - \alpha_t W_{trib,i}, if W_{trib,i} > 0 \\ W_{original,i}(1-\alpha_b), if W_{trib,i} = 0 \wedge B_i = 1 \\ W_{original,i}, if W_{trib,i} = 0 \wedge B_i = 0 \end{cases} \quad (1)$$

where $\alpha_t = 1.0$ is the tributary influence coefficient, and $\alpha_b = 0.5$ is the bridge reduction coefficient. When tributary width information was available, the tributary-related reduction was applied directly; otherwise, bridge-affected reaches were represented by a 50 % reduction of the original width. The bridge and tributary coefficients are introduced as simplified operational parameters that consistently represent local channel constrictions across all reaches. These values follow the conceptual framework of De Munck et al. (2017) and are not fully calibrated hydraulic parameters. No formal sensitivity analysis was conducted; therefore, their influence on reach-scale classification should be interpreted within a screening-level context.

The Narrowing Index (*NI*) was then computed by comparing the modified width of a reach with an upstream reference width representative of the nearest local widening condition. Rather than using a purely global maximum width, the implemented algorithm identifies widening reaches along the longitudinal profile and propagates the most recent upstream widening width downstream as the reference value. Denoting this propagated reference width for reach i as $W_{narrowing,i}$, the Narrowing Index is defined as:

$$NI_i = \frac{W_{modified,i}}{W_{narrowing,i}} \quad (2)$$

with $0 < NI_i \leq 1$. Lower values indicate stronger narrowing and, therefore, a higher predisposition to ice accumulation. Consistent with the implementation, NI_i is set to 1.0 when the current reach is wider than the immediately preceding reach, indicating that no effective narrowing is present at that location. This formulation provides a longitudinally consistent representation of local channel contraction relative to upstream widening conditions rather than to a river-wide average width.

For subsequent aggregation within the Ice Jam Predisposition Index, *NI* was discretised into four ordinal classes using fixed thresholds that were common to all rivers. Reaches with $NI < 0.54$ were assigned to class 3, those with $0.54 \leq NI < 0.75$ to class 2, those with $0.75 \leq NI < 0.92$ to class 1, and those with $NI \geq 0.92$ to class 0. This classification ensures that the strongest width contractions receive the highest predisposition score. Although localised constrictions can increase flow velocity and facilitate ice transfer under some circumstances, the present framework interprets narrowing monotonically as a factor that increases the likelihood of ice arrest and jam initiation, which is consistent with the model's overall screening objective.

2.4.2 Sinuosity index (SI)

Channel sinuosity is a key geomorphological factor influencing ice-jam formation, given that curvature in the river planform modifies flow structure, velocity distribution, and ice-transport dynamics. In meandering channels, centrifugal forces induce transverse gradients in water depth and velocity, leading to asymmetric flow conditions that can disrupt the downstream movement of ice floes and promote localised accumulation (Lucie et al., 2017). Flow curvature at bends may also increase water levels and generate zones of reduced velocity along the inner bank, further favouring ice retention and consolidation (Zhao et al., 2021). Repeated ice accumulation at bends can also alter channel morphology over time, for example, by forming scour holes and local erosion patterns in meandering reaches. In sharply curved sections, ice-induced obstructions may force flow diversion across the floodplain, particularly under high-discharge conditions (Smith and Pearce, 2002). Both numerical simulations and field observations indicate that increasing sinuosity is generally associated with higher ice-jam frequency and severity, highlighting its importance for both flood hazard assessment and sediment transport processes (Kozlov and Kuleshov, 2019).

Despite this well-established influence, the present model adopts a simplified representation of sinuosity effects. It does not explicitly account for the increased probability of ice-jam initiation at the first bend of a meandering sequence, as has been observed under certain field conditions. Instead, sinuosity is treated as a reach-scale geometric descriptor that captures the overall degree of channel curvature without resolving detailed flow ice interactions at individual bends.

Sinuosity was quantified using the Frazil toolbox (Gauthier et al., 2008), which computes a standardised sinuosity coefficient (*SV*) based on the Sinuosity4 formulation that was proposed by Dutton (1999). The coefficient *SV* is defined as the ratio between the curvilinear channel length and the corresponding straight-line distance between two points along the channel:

$$SV = \frac{L_{curve}}{L_{straight}} \quad (3)$$

where L_{curve} is the along-channel distance following the river centreline, and $L_{straight}$ is the Euclidean distance between the same two endpoints. By definition, $SV \geq 1$, with values approaching 1 corresponding to nearly straight reaches.

To obtain a normalised sinuosity measure (*SI*) bounded between 0 and 1, the following transformation was applied:

$$SI = \sqrt{1 - \frac{1}{SV^2}} \quad (4)$$

Where *SI* represents the dimensionless sinuosity index used in the present study. Under this formulation, $SI = 0$ corresponds to a perfectly straight channel, while values approaching 1 indicate highly sinuous planforms.

The computation of *SV* and *SI* is based on the identification of inflexion points along the river centreline, which delineate successive bends of opposite curvature. The distance between two consecutive inflexion points may extend over multiple adjacent 250 m reaches. In such cases, a single sinuosity value is assigned uniformly to all reaches that are encompassed within that segment. Where a given reach overlaps two sinuosity segments that were derived from adjacent inflexion-point pairs, the final *SI* value is computed as the arithmetic mean of the overlapping values. This approach ensures a consistent representation of channel curvature while preserving continuity along the longitudinal profile.

For integration into the Ice Jam Predisposition Index (*IJPI*), the continuous *SI* values were discretised into four ordinal classes {0, 1, 2, 3} using fixed thresholds that are common across all rivers. Reaches with $SI < 0.25$ were assigned to class 0, those with $0.25 \leq SI < 0.43$ to class 1, those with $0.43 \leq SI < 0.66$ to class 2, and those with $SI \geq 0.66$ to class 3. Higher classes, therefore, correspond to more pronounced channel curvature and, consequently, a greater predisposition towards ice accumulation and jam formation. While local hydraulic responses to curvature can vary with discharge, ice conditions and

https://doi.org/10.5194/egusphere-2026-2457
Preprint. Discussion started: 15 July 2026

channel geometry, sinuosity is interpreted here as a monotonic control that increases the likelihood of ice retention in curved reaches, thereby facilitating the identification of zones of elevated susceptibility.

2.4.3 Slope break index

Longitudinal variations in channel slope exert a fundamental control on river ice dynamics, particularly during break-up periods when ice mobility is strongly governed by flow velocity and hydraulic gradient. A sudden transition from a steep upstream reach to a milder downstream section reduces the flow's capacity to transport ice, thereby promoting ice accumulation and consolidation. As described by Beltaos (1995), ice floes travelling through high-gradient reaches can abruptly decelerate upon entering flatter sections, leading to increased floe interaction, enhanced interlocking, and eventual jam formation. Similarly, Kowshal et al. (2021) emphasised that such slope transitions represent preferential locations for the initiation of stable ice covers and mechanical jams, especially under conditions of high ice supply and declining flow competence.

In the present study, slope is treated as a reach-scale geomorphological descriptor that is derived directly from the digital elevation model (DEM). For each river segment *i*, the local slope magnitude was calculated using the elevation difference between the upstream and downstream endpoints of the reach. Denoting $Z_{up,i}$ and $Z_{down,i}$ as the corresponding elevations and L_i as the reach length, the slope expressed as a percentage is given by:

$$S_i = \frac{|Z_{up,i} - Z_{down,i}|}{L_i} \times 100 \quad (5)$$

where S_i represents the percent slope of reach *i*. This formulation provides a consistent, scale-independent estimate of the local channel gradient, suitable for comparison across rivers of varying size and morphology.

In addition to slope magnitude, a diagnostic variable representing slope transitions between consecutive reaches was computed. This slope-break indicator is defined as the positive decrease in slope between a reach and its immediate upstream neighbour, i.e., it is non-zero only when the downstream reach is flatter than the upstream reach. Such transitions are conceptually associated with zones of rapid deceleration and increased likelihood of ice accumulation. Yet, in the current implementation, this slope-break variable is retained solely for diagnostic and interpretative purposes and is not explicitly included in the aggregation of the Ice Jam Predisposition Index (*IJPI*). This decision reflects the objective of maintaining a parsimonious model structure while avoiding redundancy with the slope magnitude itself, which already captures first-order variations in channel gradient.

For integration into the index framework, the continuous slope values S_i were discretised into four ordinal classes {0, 1, 2, 3} using fixed thresholds common across all study rivers

Reaches with $S_i < 0.04$ were assigned to class 3, those with $0.04 \leq S_i < 0.41$ to class 2, those with $0.41 \leq S_i < 4.03$ to class 1, and those with $S_i \geq 4.03$ to class 0. Under this classification scheme, flatter reaches receive higher class values, reflecting their reduced transport capacity and greater predisposition towards ice accumulation. Conversely, steep reaches are assigned lower classes, given that higher gradients generally favour efficient ice conveyance and reduce the likelihood of jam formation.

https://doi.org/10.5194/egusphere-2026-2457
Preprint. Discussion started: 15 July 2026

Slope-break zones are widely recognised as critical controls on ice-jam initiation, but the present model interprets slope primarily through its absolute magnitude rather than through explicit transition metrics. This simplification ensures consistency with the index's overall structure while preserving the dominant influence of channel gradient on ice transport processes. Future developments of the model may explicitly integrate slope-break effects as an additional predictor to better capture localised transitions in hydraulic conditions.

2.4.4 Presence of Rapids

Abrupt variations in channel slope, particularly those that are associated with rapids, play a vital role in controlling ice dynamics along river profiles. Rapids are typically characterised by steep gradients, high flow velocities, and increased turbulence, all of which collectively enhance the flow's capacity to transport ice downstream and reduce the likelihood of local ice accumulation. Under such conditions, ice floes are less likely to consolidate or interlock, thereby limiting the formation of stable ice covers within the rapid itself. Consequently, reaches containing rapids are generally considered unfavourable locations for ice-jam initiation.

Yet the geomorphological transition immediately downstream of rapids often creates conditions highly conducive to ice-jam formation. As flow exits a steep, high-energy reach and enters a milder-gradient section, a rapid reduction in velocity and transport capacity occurs. This deceleration promotes the accumulation of incoming ice, particularly when large volumes of ice are delivered from upstream. Beltaos (2008b) explains that transitions in channel slope often act as preferred locations for ice jam formation, as the resulting decrease in hydraulic capacity promotes ice retention and enhances mechanical interactions between ice floes.

In the present model, the influence of rapids on jam formation is incorporated through a deterministic, rule-based adjustment applied after the computation of the geomorphological indices. When a reach contains rapids, its predisposition level is set to "Low", reflecting the high transport capacity and reduced likelihood of ice accumulation under steep, turbulent conditions. Conversely, the reach immediately downstream of a rapid is assigned a predisposition level of "High" to reflect the increased probability of ice-jam formation associated with abrupt slope reduction and flow deceleration.

This simplified representation does not explicitly quantify the magnitude of slope transitions or hydraulic changes; rather, it encodes their dominant effect through a spatially structured rule. While this approach enhances the model's ability to capture known ice-jam hotspots, it also introduces a heuristic component that complements the continuous geomorphological indices that are described above.

3 Data and Model Development

3.1 Database of Documented Ice Jams

Historical ice-jam occurrences were obtained from the public shapefile dataset "Historique (publique) d'embâcles répertoriés au MSP", provided by the Ministère de la Sécurité publique du Québec (MSP) through Données Québec (MSP, 2024). This

https://doi.org/10.5194/egusphere-2026-2457
Preprint. Discussion started: 15 July 2026

dataset represents the most comprehensive provincial inventory of documented ice-related flood events in Quebec. It compiles information from municipal and governmental reports submitted in both digital and paper formats and typically includes the affected water body, approximate geographic location, date of occurrence, type of ice event, such as break-up, freeze-up, or unspecified events, a description of impacts, and the source of information.

The dataset used in this study covers documented ice-jam events from 1985 to 2023 and was accessed during data compilation in 2024. However, the consistency of the observational record varies over time. Records prior to about 2005 were primarily based on opportunistic reporting by human observers and heterogeneous information sources, which may have introduced temporal inconsistencies in data collection. In contrast, monitoring practices became more systematic and standardized after 2005, improving the reliability and completeness of the dataset. These differences in observation methods are common in environmental monitoring and may introduce temporal biases in historical event inventories.

The reliance on opportunistic reporting also introduces spatial biases, as events in populated or infrastructure-rich areas are more likely to be detected and documented than those in remote or sparsely inhabited river reaches. Consequently, the absence of a recorded event at a given location does not necessarily indicate the absence of an ice jam, given that the probability of recording an event depends not only upon its actual occurrence, but also on the likelihood of its observation and reporting (Arsenault-Boucher et al., 2026). Factors such as site accessibility, proximity to populated areas, and monitoring intensity can influence the completeness of historical inventories. These observational and reporting biases are consistent with challenges reported in other ice-jam inventories and opportunistic environmental datasets (Arp et al., 2024; Beltaos, 2023; McPherson and Myers, 2009; Neary et al., 2023).

Additional uncertainties arise from the accuracy of the recorded events' locations. Because ice jams often extend over long river reaches, the coordinates that are provided in the MSPQ database generally represent approximate locations and may not correspond to the exact initiation point (e.g., the toe of the jam). Furthermore, some entries may refer to related ice processes, such as anchor ice or frazil accumulations, rather than fully developed surface jams (Madaeni et al., 2022).

To enhance data reliability, events with insufficient locational accuracy or ambiguous descriptions were excluded from the analysis. Moreover, to account for potential spatial offsets between recorded and actual initiation points, river reaches adjacent to documented locations were included in the validation process. After applying these quality-control procedures, a total of 649 well-documented ice-jam events were retained for use in model development and validation.

3.2 Index framework and post-classification rules

Geomorphological controls influencing ice-jam formation often operate over spatial scales comparable to, or slightly larger than, the adopted reach length. Local features such as bends, channel constrictions and bridge-affected sections modify hydraulic conditions over short distances, with their influence typically extending into adjacent upstream and downstream reaches. In addition, uncertainties in reach segmentation and in the geolocation of historical ice-jam events, commonly on the order of 100-300 m, may lead to spatial offsets between mapped predisposition peaks and actual initiation locations.

https://doi.org/10.5194/egusphere-2026-2457
Preprint. Discussion started: 15 July 2026

Furthermore, stable ice arches rarely initiate within rapids, where high flow velocity and turbulence enhance ice transport capacity. Instead, initiation is more frequently observed immediately downstream of rapids, where slope and velocity decrease abruptly (Beltaos, 1995; Kowshal et al., 2021).

To account for these spatial effects, a set of deterministic post-classification rules was introduced to complement the geomorphological indices. These rules are designed to enforce longitudinal continuity of predisposition and to suppress unrealistic, high-susceptibility predictions within hydraulically unfavourable zones, such as rapids.

Geomorphological predisposition is initially quantified using three primary indices: narrowing (*NI*), sinuosity (*SI*), and slope, while the presence of rapids is incorporated as a rule-based hydraulic control. These indices are aggregated into the Ice Jam Predisposition Index (*IJPI*), which is subsequently classified into three susceptibility levels: LOW, MED, and HIGH.

Following the initial classification, a neighbour-adjustment rule is applied, whereby any reach that is classified as high increases the class of its immediate upstream and downstream neighbours by one level (i.e., LOW → MED, MED → HIGH), with values capped at HIGH. This operation accounts for the spatial propagation of hydraulic effects and reduces the model's sensitivity to segmentation artefacts.

A rapid-based adjustment is then applied. Reaches identified as containing rapids are assigned to a low predisposition, reflecting their high transport capacity and reduced likelihood of ice accumulation. Conversely, the reach immediately downstream of each rapid is assigned a high predisposition, consistent with the increased likelihood of ice-jam initiation at locations of abrupt slope reduction and flow deceleration. The sequential application of the neighbour-adjustment rule, followed by the rapids rule, is consistent with the model's operational implementation.

This study extends the *IJPI* framework through fully automated geospatial processing and its consistent application across 35 rivers in southern Quebec. Structural and geomorphological features such as bridges, tributaries, and islands are incorporated indirectly through dynamic width adjustments in the Narrowing Index, while rapids are explicitly represented as localised hydraulic controls. The framework is further supported by validation against an expanded, spatially refined dataset of documented ice-jam events, thereby enhancing both its robustness and operational applicability.

3.3 Classification of Index Values

The three continuous predictors, narrowing index (*NI*), sinuosity index (*SI*), and slope, are discretised into four ordinal classes {0, 1, 2, 3} using fixed thresholds applied uniformly across all rivers. This harmonised classification ensures comparability across rivers with varying sizes and morphologies, while maintaining consistency with the operational GIS implementation.

Class assignment follows the physical interpretation of each variable. Lower *NI* values indicate stronger channel constriction and are therefore associated with higher classes. Higher *SI* values reflect greater channel curvature and correspond to higher class assignments. Lower slope values indicate flatter reaches with reduced transport capacity and are likewise associated with higher classes, consistent with increased predisposition to ice accumulation.

Table 1. Fixed thresholds (t_i) for class discretisation (0–3)

https://doi.org/10.5194/egusphere-2026-2457
Preprint. Discussion started: 15 July 2026

Index (units)	t_1	t_2	t_3	**Class direction**
NI **(–)**	0.54	0.75	0.92	lower = higher class
SI **(–)**	0.25	0.43	0.66	higher = higher class
Slope (%)	0.04	0.41	4.03	lower = higher class

The thresholds used to discretise *NI*, *SI*, and slope were defined using a data-driven approach based on the statistical distribution of geomorphological index values across the study rivers. Following the *IJPI* framework, each predictor was standardised into four ordinal classes using fixed thresholds derived from a clustering analysis of the geomorphological index distributions across the study rivers. Particular attention was given to river reaches associated with frequent ice-jam occurrences, ensuring that class boundaries reflect the geomorphological conditions most conducive to ice accumulation and arrest.
Minor adjustments were introduced to account for differences in data resolution, river segmentation, and geomorphological variability across the expanded Quebec dataset. These adjustments ensure that the thresholds remain representative of the observed distributions while preserving a consistent interpretation of class ordering and physical meaning across all rivers.
This classification strategy provides a stable and transferable discretisation of geomorphological predictors, enabling consistent regional-scale comparisons while maintaining sensitivity to the underlying data structure.

3.4 Relative Weighting of Indices

To quantify the relative contribution of geomorphological predictors to ice-jam predisposition, an empirical, data-informed approach was adopted. The weighting scheme was derived by analysing the spatial correspondence between historical ice-jam occurrences and the classified values of the geomorphological indices.
More specifically, the frequency and distribution of documented ice-jam events were examined across river reaches that were characterised by different classes of narrowing, sinuosity, and slope. This cross-analysis enabled the identification of the geomorphological conditions that are most frequently associated with ice accumulation and arrest. As a result, greater importance was assigned to predictors showing stronger spatial agreement with observed ice-jam locations.
The analysis indicated that channel narrowing exhibits the strongest relationship with ice-jam occurrence, reflecting its direct control on flow constriction and ice transport capacity. Sinuosity was found to have a secondary influence, given that channel curvature modifies flow structure and promotes localised ice retention. In contrast, slope showed a more moderate effect, primarily influencing flow energy and ice mobility at the reach scale.
Based on these observations, a fixed weighting scheme was defined to represent the relative importance of each predictor in the computation of the Ice Jam Predisposition Index (*IJPI*). The adopted weights are presented in Table 2.

https://doi.org/10.5194/egusphere-2026-2457
Preprint. Discussion started: 15 July 2026

Table 2. Relative weights assigned to geomorphological indices in *IJPI* computation

Factor	Weight
Narrowing class	0.65
Sinuosity class	0.23
Slope class	0.12

Bridge and tributary effects were not treated as independent predictors in the weighting process. Instead, their influence was incorporated indirectly through modifications to the effective channel width used in the computation of the Narrowing Index. This approach ensures that local hydraulic constraints are consistently represented while avoiding redundancy among correlated variables.

The resulting weighting scheme provides a physically consistent and operationally robust representation of geomorphological controls on ice-jam formation, allowing its application across a diverse set of river systems.

3.5 Computation of the Ice Jam Predisposition Index (*IJPI*)

For each reach *iii*, the Ice Jam Predisposition Index (*IJPI*) is computed as a weighted aggregation of the three classified indices:

$$IJPI_i = \frac{w_{NI}C_{,i} + w_{SI}C_{SI,i} + w_S C_{S,i}}{3} \quad (6)$$

where $C_{NI,i}$, $C_{SI,i}$, and $C_{S,i}$ are the class values (0–3) that are associated with narrowing, sinuosity and slope, respectively, and w_{NI}, w_{SI}, and w_S are their corresponding weights (0.65, 0.23, and 0.12). The denominator (3) ensures consistency with the operational implementation and normalises the index to a bounded range.

The resulting *IJPI* values are rounded to two decimal places and mapped to three susceptibility categories using fixed thresholds: LOW for $IJPI < 0.40$, MED for $0.40 \leq IJPI < 0.54$, and HIGH for $IJPI \geq 0.54$. These thresholds were selected to balance sensitivity and interpretability in identifying reaches that are prone to ice-jam formation.

Figure 4 illustrates the overall workflow of the *IJPI* computation, from the extraction of geomorphological attributes (river geometry, tributaries, bridges, islands, and rapids) to the derivation of individual indices and their aggregation into the final predisposition map.

https://doi.org/10.5194/egusphere-2026-2457
Preprint. Discussion started: 15 July 2026

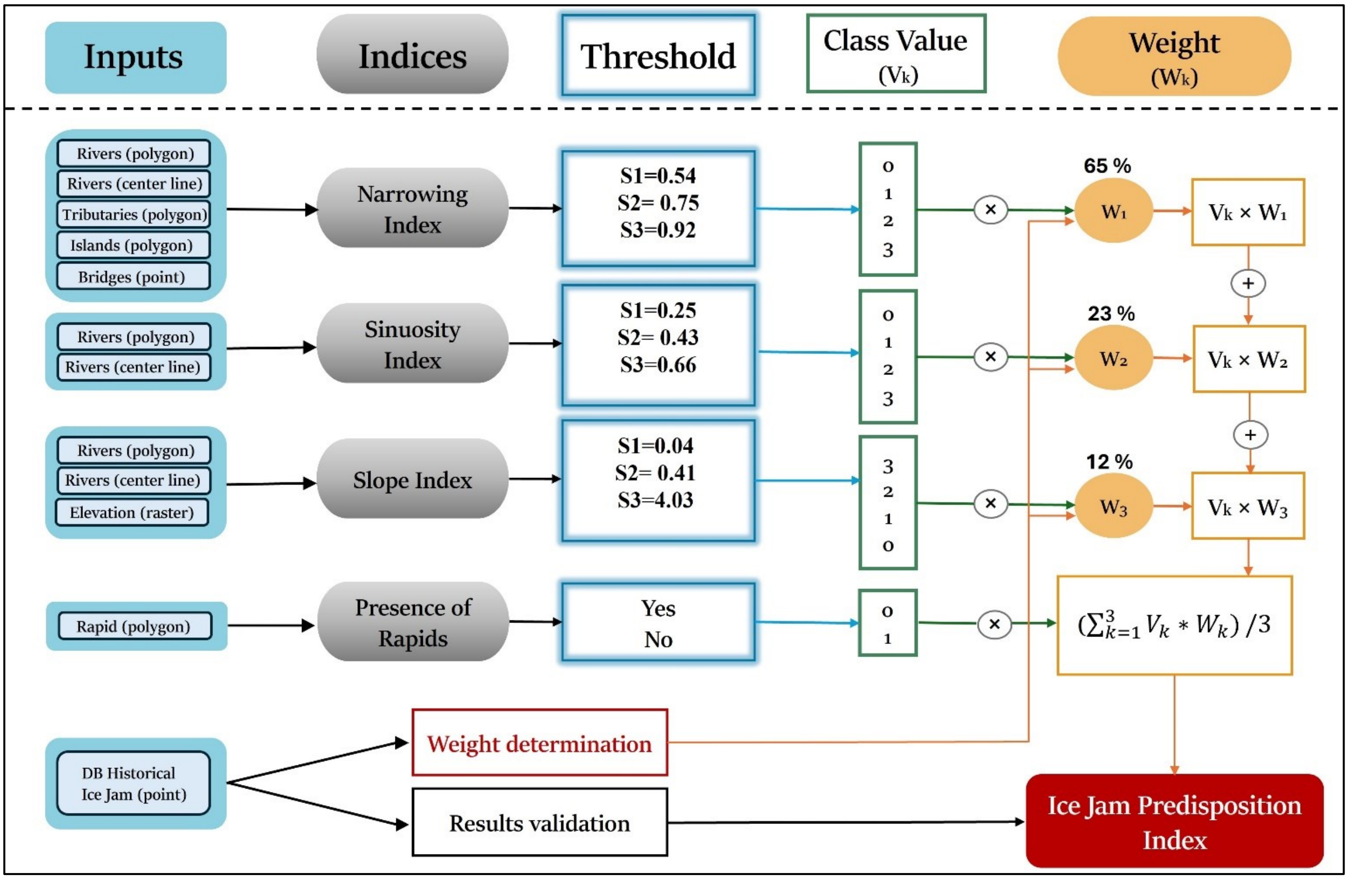

Figure 4: Schematic representation of the model illustrating factors influencing ice jam susceptibility.

Model performance was evaluated at the reach scale by intersecting documented ice-jam locations with the classified river segments using a spatial join. Reaches that were classified as MED or HIGH were considered positive predictions, whereas LOW class reaches were treated as negative. Performance was then quantified using recall and precision, defined as:

$$Recall = \frac{TP}{TP+FN} \quad (7)$$

$$Precision = \frac{TP}{TP+FP} \quad (8)$$

where TP is the number of documented ice-jam events located within reaches classified as MED or HIGH predisposition, FN is the number of documented events located within reaches classified as LOW, and FP is the number of MED- or HIGH-classified reaches containing no documented ice-jam event. Evaluation focused primarily on recall because the primary objective of the framework is to support flood-risk management, where failing to identify a jam-prone reach (a false negative) is a more critical outcome than overestimating susceptibility.

https://doi.org/10.5194/egusphere-2026-2457
Preprint. Discussion started: 15 July 2026

Precision was also examined to assess model behaviour more fully; in this framework, lower precision values reflect a conservative prediction strategy in which a larger number of reaches are classified as susceptible. While this increases the rate of false positives, it ensures that most hazardous locations are captured, consistent with the model's intended use as a screening and early-warning tool.

In addition to these metrics, the spatial distribution of observed ice jams across susceptibility classes was analysed to assess model performance further. All evaluation steps were conducted consistently within the modelling framework, including the use of modified widths for narrowing computation, fixed thresholds and classification weights, and the application of neighbour-adjustment and rapid rules during post-processing.

4 Results and Discussion

4.1 Model Performance Across all Rivers

The geomorphological predisposition model was evaluated across 35 rivers in southern Quebec to assess its ability to identify river reaches that were prone to ice-jam formation. Figure 5 presents the recall values that were obtained for each river, while Figure 6 summarises the corresponding true-positive (TP) and false-negative (FN) counts, together with the number of observed ice-jam events. Overall, the model achieved a mean recall of 0.90, with values ranging from 0 to 1.00. This high average recall indicates that the model successfully detects most ice jam-prone reaches across the study region. The original *IJPI* model reported that approximately 77 % of observed ice-jam events occurred within river sections classified as having medium to high predisposition across the three study rivers. In comparison, the present model achieves a higher overall recall across a larger dataset of 35 rivers, indicating an improved overall performance.

https://doi.org/10.5194/egusphere-2026-2457
Preprint. Discussion started: 15 July 2026

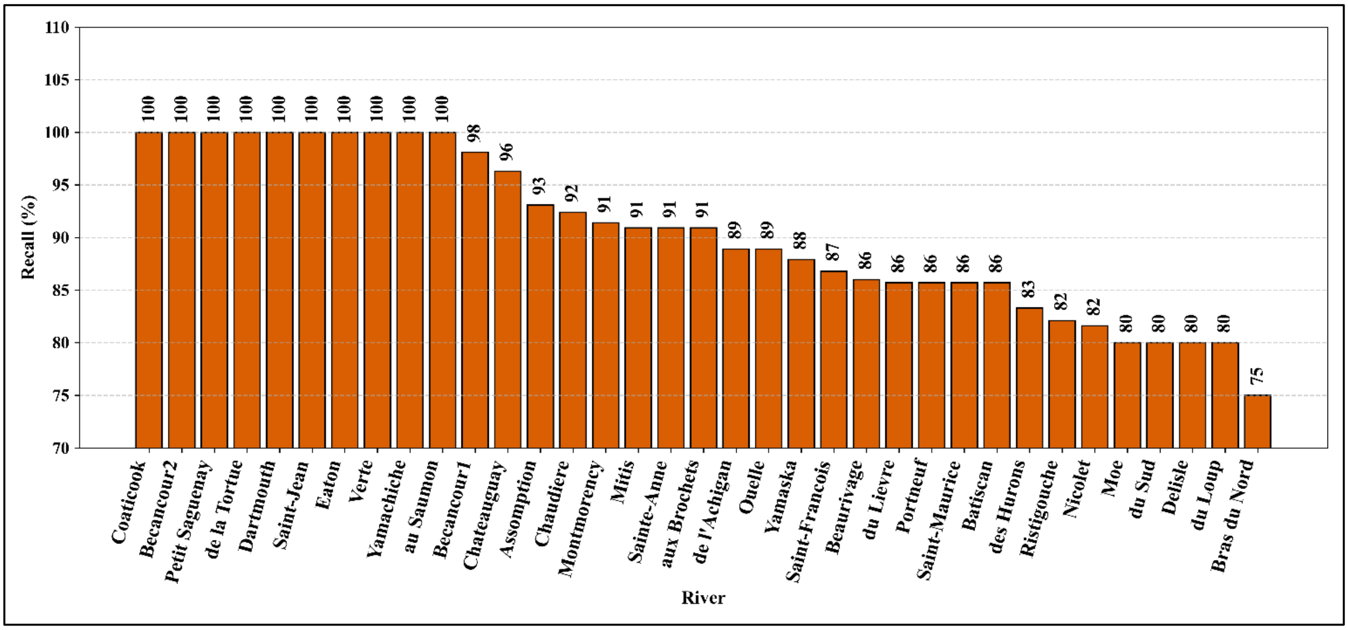

Figure 5: Model Recall (%) Across the 35 Quebec River.

Among the available evaluation metrics, recall is the most relevant for assessing geomorphological models of ice jam predisposition. In this context, a false negative, i.e., a location that is prone to jamming but classified as low risk, represents a much more serious outcome than does a false positive. Missing a positive case can result in unanticipated flooding, property damage, and potential threats to public safety. Therefore, maximising recall ensures that nearly all potentially hazardous reaches are identified within the High and Medium predisposition classes, even if this approach slightly increases the number of non-hazardous reaches that were included. The model is thus intentionally conservative, prioritising risk detection over spatial precision, which aligns with the preventive objectives of flood-risk management agencies such as the MSPQ.

As shown in Figure 5, most rivers exhibit recall values exceeding 80 %, indicating the robustness and transferability of the model across diverse geomorphological and hydrological settings. Several rivers, including the Chaudière, St-François, L'Assomption, and Bécancour, achieved recall values close to 100 %, indicating that all known ice-jam occurrences were successfully captured within the predicted High or Medium predisposition reaches. Only a limited number of rivers recorded recall values below 80 %. These were typically waterways with very few historical events or those whose channels have undergone anthropogenic modifications, e.g., levees, straightening, or unaccounted for bridges. Such variability reflects the natural complexity of river systems but also demonstrates that the model performs consistently across contrasting environments.

The model was designed to be conservative, but the false-positive predictionsremained relatively low across all rivers, indicating that the expansion of High and Medium predisposition zones did not lead to excessive over-prediction. This balance

https://doi.org/10.5194/egusphere-2026-2457
Preprint. Discussion started: 15 July 2026

between broad hazard coverage and acceptable overestimation supports the model's suitability for large-scale screening and early-warning applications.

It is important to note that some of the false-positive (FP) predictions may be partially attributable to limitations in the historical ice-jam inventory rather than to deficiencies in the geomorphological model itself. As described in Sect. 3.1, the MSPQ database relies on a combination of municipal reports, media sources, and observer accounts, particularly for earlier years, which introduces spatial and temporal reporting biases. Ice-jam events occurring in remote or sparsely populated river reaches may therefore remain undocumented due to limited observation effort. Consequently, reaches that are classified by the model as having medium or high predisposition but lack recorded events should not necessarily be interpreted as true prediction errors. Instead, these locations may represent previously unrecognised or underreported ice-jam-prone areas, thereby supporting the model's role as a proactive screening tool for identifying sites that warrant further monitoring and field verification.

Analysis of false-negative sites shows that most occur along reaches characterised by abrupt slope transitions or local morphological discontinuities. These localised discrepancies may also be influenced by the use of fixed-length (250 m) river segments, which may not fully capture the natural spatial variability of geomorphological controls on ice-jam formation, despite being operationally consistent for regional-scale analysis. Ice jams frequently develop at discrete morphological transitions, such as abrupt channel narrowing, changes in sinuosity or slope, or the presence of structural and confluence features. Consequently, segmentation approaches that are based on natural breaks in these key parameters could provide a more physically meaningful representation of river reaches and improve the spatial accuracy of predisposition mapping. The exploration of such natural, parameter-based segmentation constitutes a promising direction for future research and provides the basis for ongoing work aimed at further refining the *IJPI* framework.

In these cases, the combined effect of the narrowing and sinuosity indices, together with the use of fixed-length segmentation, may under-represent rapid local constrictions, leading to occasional omissions. Nevertheless, the overall recall distribution confirms that the refined approach, including width corrections for bridges and tributaries and the neighbouring-segment adjustment, substantially improves the spatial coherence of high-predisposition zones. Consequently, the model provides a reliable geomorphological screening tool for identifying ice jam-prone reaches at the regional scale.

The spatial validation results highlight strong correspondence between the modelled predisposition zones and the locations of observed ice-jam events across the 35 Quebec rivers. Figure 6 illustrates the distribution of true positives (TP) and false negatives (FN) that were obtained for each river. In most cases, the number of TPs exceeds that of FNs, confirming that the model successfully identifies most ice-jam-prone reaches. Several rivers exhibit only true detections, with no missed events, indicating perfect spatial agreement between observed and predicted sites.

https://doi.org/10.5194/egusphere-2026-2457
Preprint. Discussion started: 15 July 2026

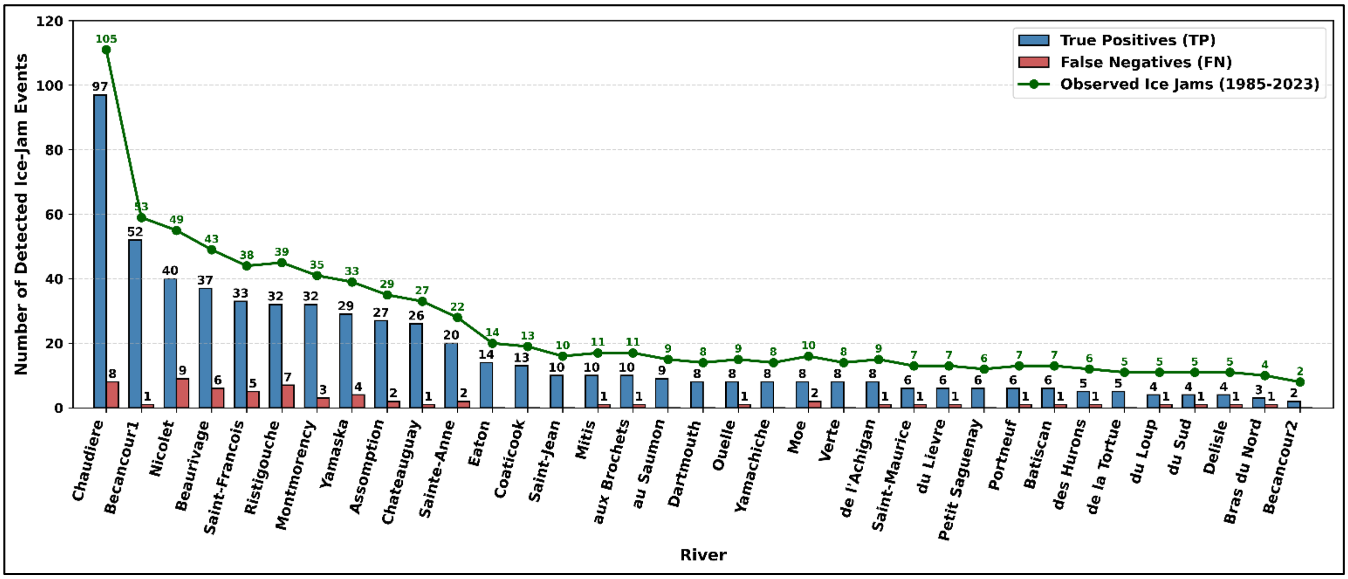

Figure 6: True positives (TP) and false negatives (FN) across 35 southern Quebec rivers, with the green line showing observed ice-jam events (1985–2023).

The few false negatives recorded are generally isolated and spatially localised rather than being encountered systematically along an entire river. Their occurrence tends to be associated with geomorphological transitions, such as slope breaks, confluences, or short segments that are characterised by strong local heterogeneity. In some reaches, field observations of ice-jam locations were slightly displaced from the actual formation zones, often being recorded a few hundred metres upstream of where the jam had initiated. This spatial shift can cause some observed points to fall within adjacent low-risk reaches, even though the actual ice-jam formation site lies in the neighbouring high-predisposition segment. Such displacement reflects both the dynamic nature of ice-jam propagation and the inherent positional uncertainty in historical event databases.

In some cases, such as the Montmorency River, false negatives were found within segments containing rapids, which are normally classified as low predisposition due to high flow velocities. Yet, closer examination revealed that where strong narrowing occurs within or immediately downstream of rapid zones, ice jam formation remains possible, suggesting that the narrowing factor can dominate the hydraulic effect of rapids. These cases emphasise the importance of local morphological context and highlight how interactions among geomorphological parameters can locally override generalised predisposition rules.

Overall, spatial validation confirms that the updated model captures the dominant geomorphological controls on ice-jam occurrence at the regional scale. The small proportion of false negatives demonstrates that integrating bridge and tributary corrections, along with the neighbourhood adjustment rule, has improved the model's capacity to delineate contiguous high predisposition reaches. These findings validate the model's robustness for large-scale screening and provide confidence in its use for spatial prioritisation of monitoring and field verification efforts.

https://doi.org/10.5194/egusphere-2026-2457
Preprint. Discussion started: 15 July 2026

4.2 Dominant Geomorphological Drivers of Ice-Jam Formation

To better understand the geomorphological conditions that are associated with ice-jam formation, the frequency of key geomorphological and structural parameters was analysed for all river reaches intersecting documented ice-jam events. This analysis aims to identify the dominant morphological drivers of ice-jam predisposition across the studied river network. Table 3 summarises the frequency of key geomorphological and structural parameters within the 432 reaches intersecting recorded ice-jam events across the 35 study rivers.

By integrating both medium and high-class conditions (Class ≥ 2), the analysis captures the full continuum of morpho-dynamical predisposition described in the *IJPI* formulation.

The results highlight flat slopes (85 %) as the overwhelmingly dominant control on ice-jam formation, confirming that reduced hydraulic energy and prolonged ice residence time are the main enablers of blockage formation. Sinuosity (49 %) and narrowing (31 %) act as strong secondary factors, reflecting the combined influence of planform curvature and cross-sectional confinement on channel hydraulics. Bridges (16 %) appear as recurrent local amplifiers, which are often superimposed on geomorphologically sensitive meanders. Tributary confluences (3 %), though spatially limited, contribute to local backwater and dynamic shear zones that favour accumulation. Steep reaches that are characterised by rapids were identified in only (1.4 %) of the jam-intersecting segments, confirming their inhibitory role in ice accumulation. These results further support the assumption that rapids, characterised by higher flow velocities and increased turbulence, significantly reduce the likelihood of ice-jam formation. Consequently, classifying reaches with rapids as low-risk segments, while assigning higher risk to the downstream segments where slope breaks occur, appears to be a sound modelling decision. Nevertheless, six segments exhibited ice-jam events despite the presence of rapids, representing false negatives (FNs). A closer examination of these cases revealed that two segments had a sinuosity class greater than 2, and two others had a narrowing class greater than 2, indicating that additional geomorphological constraints may locally override the inhibitory effect of rapids. Among the remaining segments, one was located near a bridge, suggesting the influence of anthropogenic structures, while the other was situated within 100 metres of an adjacent segment, which may reflect spatial uncertainty in the observational data. Overall, this analysis reinforces the robustness of the modelling approach while highlighting the multifactorial nature of ice-jam formation.

Overall, these frequencies confirm that reduced slope, enhanced sinuosity, and cross-sectional confinement are the main geomorphological controls governing ice-jam predisposition in Quebec rivers, in agreement with the *IJPI* model's weighting structure.

https://doi.org/10.5194/egusphere-2026-2457
Preprint. Discussion started: 15 July 2026

Table 3. Proportion of predisposing geomorphological and parameters in ice-jam-intersecting segments.

Factor	Variable Condition	Count (n)	% of Total (n = 432)
Narrowing	Narrowing Class ≥ 2	135	31.3 %
Sinuosity	Sinuosity Class ≥ 2	212	49.1 %
Flat Slope	Slope Class ≥ 2	368	85.2 %
Tributary Confluence	Tributary = 1	15	3.5 %
Bridge	Bridge = 1	70	16.2 %

The present analysis explores how these factors combine across the 432 river reaches that intersect observed ice jam events. Ice jam formation rarely arises from a single controlling variable; instead, it reflects the compound influence of multiple predisposing conditions acting simultaneously.

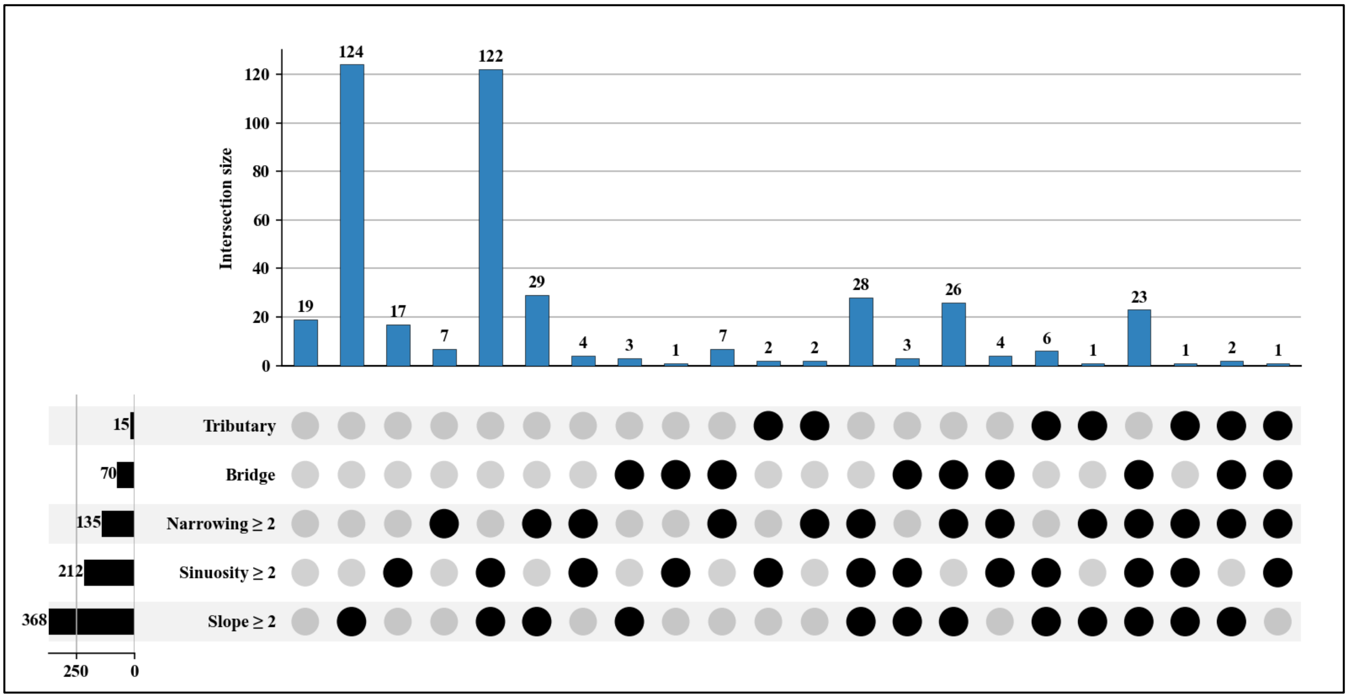

Figure 7: UpSet plot (Lex et al., 2014) showing the frequency and co-occurrence of geomorphological and structural factors associated with ice-jam-prone river segments in Quebec. The top bars indicate intersection sizes, the lefthand bars represent individual factor frequencies, and the dot matrix displays the corresponding factor combinations.

https://doi.org/10.5194/egusphere-2026-2457
Preprint. Discussion started: 15 July 2026

Figure 7 presents all significant combinations among the five main predisposing factors: Narrowing (≥ 2), Sinuosity (≥ 2), Slope (≥ 2), Bridge, and Tributary.

The figure shows that more than 60 % of jam-prone reaches exhibit at least two concurrent predisposing factors, confirming the multifactorial nature of ice-jam formation. The dominant combinations involve a flat slope with high sinuosity and narrowing, corresponding to confined meander belts where curvature and reduced gradient jointly favour ice retention. Intersections, including bridges or tributaries, further enhance local predisposition, illustrating how anthropogenic and natural constrictions can compound geomorphic risk.

Overall, the co-occurrence analysis demonstrates that ice jams in southern Quebec typically emerge from the interaction of multiple geomorphological controls rather than from isolated conditions. This emphasises the need to consider combined factor effects in future model calibration and risk-mapping workflows.

Taken together, the frequency and co-occurrence analyses confirm that ice-jam predisposition results from the combined effect of several geomorphological and structural factors, primarily low slope, high sinuosity, and narrowing. These interdependent conditions create confined, low energy reaches where ice accumulation is most likely to initiate. The following section illustrates these general findings through a detailed analysis of the Chaudière River, providing a representative example of how the identified geomorphological drivers manifest at the river scale.

4.3 Chaudière River Case Study

To illustrate how the dominant geomorphological drivers identified at the regional scale manifest in a real-world context, the Chaudière River was selected as a representative case study. This river exhibits a high frequency of documented ice-jam events and encompasses a wide range of predisposing conditions, making it an ideal example for examining the spatial expression and predictive performance of the proposed geomorphological model.

This river, in southern Quebec, has historically experienced recurrent ice-jam flooding, particularly in the Beauceville and Saint-Georges corridors, where channel confinement and human infrastructure amplify the risk of ice accumulation. Owing to the large number of recorded events and its well-documented morphology, the Chaudière offers an ideal benchmark for validating the refined model and comparing its performance with the earlier version developed by De Munck et al. (2017).

https://doi.org/10.5194/egusphere-2026-2457
Preprint. Discussion started: 15 July 2026

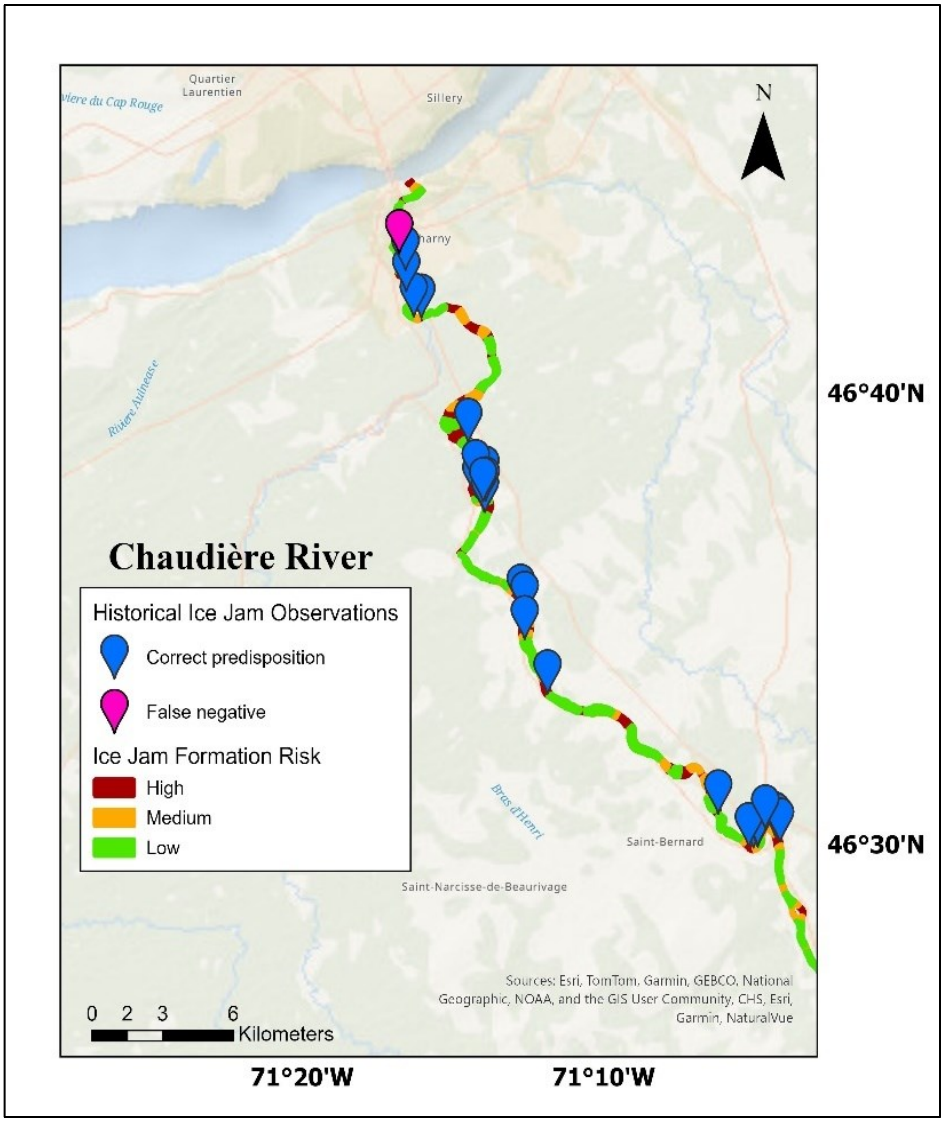

Figure 8: Spatial validation map for the Chaudière River, showing the spatial agreement between historical ice-jam observations and the predicted ice-jam formation risk classes along the river reaches. Blue markers indicate observed ice-jam locations falling within reaches classified as medium or high risk, whereas the pink marker indicates an observed ice-jam location falling within a low-risk reach. Map created by the authors using ArcGIS from historical ice-jam records and geospatial datasets compiled for this study. Sources: Esri, TomTom, FAO, USGS | Powered by Esri.

Figure 8 presents the spatial validation map for the Chaudière River, showing the predicted predisposition classes (High, Medium, and Low) and the locations of observed ice-jam events. The spatial correspondence is striking; nearly all observed ice jams fall within or are immediately adjacent to the predicted High and Medium reaches, while Low segments remain largely

https://doi.org/10.5194/egusphere-2026-2457
Preprint. Discussion started: 15 July 2026

unaffected. The model successfully delineates areas of high predisposition where multiple geomorphological risk factors, such as channel narrowing, increased sinuosity, numerous bridges and islands, favour local ice accumulation and flow deceleration. The model achieved a recall of 0.92 and a precision of 0.23, indicating that most observed events fall within the predicted High or Medium domain. This high sensitivity is essential for preventive risk screening, ensuring that potentially hazardous areas are not overlooked, even if some low-risk segments are over-classified. The confusion-matrix analysis suggests that true detections dominate over misclassifications, indicating that omission errors remain limited and that the classification is overall robust.

On the Chaudière River, the proposed model achieves a recall of 0.92, compared to 0.86 reported for the original *IJPI* model. This improvement suggests potential gains in identifying ice-jam-prone reaches under the present framework, although some of these differences may be influenced by variations in data availability and preprocessing.

Of 829 segments along the Chaudière, 437 (52.7 %) were classified as Low, 181 (21.8 %) as Medium, and 211 (25.5 %) as High predisposition. Among the 105 recorded ice jam events, 53 occurred in High, 44 in Medium, and only 8 in Low predisposition reaches, indicating that more than 90 % of the observed events were located within the predicted High–Medium domain. This strong correspondence supports that the geomorphological weighting scheme, particularly the dominance of channel narrowing, provides a consistent representation of the dominant physical mechanisms underlying ice-jam initiation along the Chaudière River.

The eight false negatives identified along the Chaudière River are confined to specific geomorphological transition zones, such as local slope breaks, tributary junctions, or segments adjacent to rapids. Two of these false negatives occur within segments containing rapids, yet in both cases the local morphology explains their classification. In one segment, a pronounced channel narrowing immediately downstream of the rapid likely promoted ice accumulation despite the high velocities typically associated with rapids. In the other, the jam was recorded near the downstream end of a rapid, intersecting a high-risk reach that was characterised by a visible slope break and an abrupt reduction in gradient. These patterns suggest that reaches immediately downstream of rapids are particularly prone to ice jam formation, where flow deceleration and partial ice blockage occur after high-velocity zones.

In several locations, the observed ice jam points were recorded slightly upstream of the actual formation sites, consistent with the hydraulic backwater effect during break-up events, where flooding peaks above the point of jam initiation. This spatial offset explains why some observations coincide with Low-risk segments, even though physical conditions favour jamming in adjacent High- or Medium-risk reaches.

A similar phenomenon is observed in the Montmorency River, where ice jams occurred downstream of rapids under strong channel narrowing, again demonstrating that narrowing can locally outweigh the hydraulic influence of high-velocity zones. Together, these examples highlight the dynamic interplay of geomorphological factors and confirm that the model captures the dominant predisposing conditions even in morphologically complex reaches.

A complementary analysis of false-positive patterns further clarifies model behaviour. Roughly 7 % of the Chaudière's segments that were classified as High risk showed no recorded ice jams, and about 10 % of Medium-risk segments lacked

https://doi.org/10.5194/egusphere-2026-2457
Preprint. Discussion started: 15 July 2026

observed events. This apparent overprediction should be interpreted considering the limitations of the historical ice-jam inventory described earlier. Spatial and temporal variability in observation effort may have led to the under-reporting of events in certain reaches. Many of the segments that were identified as false positives coincide with geomorphological configurations that are physically conducive to ice accumulation. Therefore, these locations should not necessarily be considered true model errors but may instead represent latent or previously unrecognised ice-jam-prone zones, consistent with the model's conservative design and screening objective.

To further clarify the influence of structural and confluence features, Table 4 summarises the distribution of bridges, tributaries, rapids, and slope-break zones along the Chaudière and their association with model errors. This breakdown distinguishes between false-negative and false-positive occurrences and reveals how the updated model better represents localised hydraulic constraints. The table shows that only a few false negatives remain within bridge or rapid segments, whereas most false positives correspond to morphologically confined zones where jamming potential exists, but no events were recorded. This pattern confirms that the refined structural weighting scheme reduces omission errors while maintaining conservative hazard identification.

Table 4. Structural and Confluence Features Associated with Model Errors for the Chaudière River

Feature Type	Segments with Feature (n)	Segments with Ice Jams (n)	False Negatives (n)
Bridge	16	6	2
Tributary	13	6	1
Rapids	8	2	2
Slope break/transition	12	4	3
No specific feature	780	87	0
Total	829	105	8

Together, the regional assessment and the Chaudière River case study validate the effectiveness of the proposed geomorphological framework for identifying ice-jam-prone reaches. The following section summarises the key findings and their broader implications.

5 Conclusion

This study extends the geomorphological approach to ice-jam predisposition mapping developed by De Munck et al. (2017) by applying the refined model to 35 rivers across southern Quebec. The large-scale validation supports the applicability of the Ice Jam Predisposition Index (*IJPI*) for regional screening of ice-jam-prone reaches. The model achieved an average recall of about 0.9, indicating that most observed ice-jam locations were correctly identified, with over 90 % of events occurring within reaches classified as medium or high predisposition. This high sensitivity indicates that the model is effective as a conservative screening tool for identifying potentially hazardous sites, where omission errors would have severe consequences.

Beyond spatial validation, the analysis of geomorphological factors suggests that ice jams are predominantly governed by a combination of low longitudinal slope, high sinuosity, and channel narrowing, which collectively promote flow deceleration and ice accumulation. Structural elements such as bridges and tributary confluences, which were already considered in De Munck's formulation, were found to intensify local confinement and backwater effects, thereby reinforcing predisposition in otherwise stable reaches. Including rapids as an explicit variable provides additional insight into the inverse relationship between steep, high-energy morphology and jam formation, thereby contributing to a more nuanced representation of low-susceptibility zones.

The application of the refined model across 35 rivers reveals consistent geomorphological patterns across contrasting hydrological and physiographic settings, suggesting its potential for broader-scale mapping. From a management perspective, the spatial distribution of high-risk reaches derived from this analysis may help stakeholders, including the Quebec Ministry of Public Safety (MSPQ), prioritise field monitoring, infrastructure inspection, and mitigation planning.

Future work will focus on integrating geomorphological and meteorological predictors to develop a hybrid model that is capable of estimating ice-jam occurrence under specific hydroclimatic conditions. In parallel, extending the approach to climate-change scenarios will enable assessment of how evolving temperature and discharge regimes may influence the spatial distribution and recurrence of ice-jam hazards. Together, these developments may further support the use of geomorphological modelling as a proactive decision-support tool for river-ice risk management in northern regions.

Data Availability

The datasets used in this study were obtained from publicly accessible provincial data sources. Historical ice-jam observations were obtained from the public shapefile dataset "Historique (publique) d'embâcles répertoriés au MSP", provided by the Ministère de la Sécurité publique du Québec (MSP) through Données Québec (MSP, 2024). Hydrographic data, including river polygons and related hydrographic features, were obtained from the Géobase du réseau hydrographique du Québec (GRHQ), distributed through Données Québec by the Ministère des Ressources naturelles et des Forêts (MRNF, 2024). Bridge locations were extracted from the public "Structure" dataset distributed through Données Québec by the Ministère des Transports et de la Mobilité durable du Québec (MTMD, 2024). LiDAR-derived digital terrain models used for slope calculation were obtained from provincial terrain datasets distributed through Données Québec by the MRNF (MRNF, 2024). These source datasets are openly accessible through the original data providers listed in the reference section.

Author Contribution

EM conceived the study, carried out the analysis, and prepared the manuscript. RL provided the raw data and contributed to the study design. KC supervised the research and provided overall guidance. SH reviewed and edited the manuscript. All authors contributed to the interpretation of the results and approved the final manuscript.

Competing Interests

The authors declare that they have no conflict of interest.

Acknowledgments

The authors gratefully acknowledge the Ministère de la Sécurité publique du Québec (MSPQ) for providing access to the historical ice-jam database used in this study. Geospatial datasets were obtained from Données Québec via its open data platform. The authors also thank W. F. J. Parsons for revising the English text.

Financial Support

This work was supported by a doctoral scholarship awarded by the Institut national de la recherche scientifique (INRS).

References

Arp, C. D., Bondurant, A. C., Clement, S., Eidam, E., Langhorst, T., Pavelsky, T. M., Davis, J., and Spellman, K. V.: Observation of high sediment concentrations entrained in jumble river ice, River Res. Appl. (40), 1560–1570, https://doi.org/10.1002/rra.4309, 2024.

Arsenault-Boucher, L., Boucher, É., Lhissou, R., Chokmani, K., and Kinnard, C.: Addressing Biases in Ice Jam Observations by Integrating Multi-Source Data in a Forested Fluvial Landscape, Southern Quebec, River Res. Appl., https://doi.org/10.1002/rra.70133, 2026.

Beltaos, S.: River ice jams, Water Resources Publications, LLC, 390, 1995.

Beltaos, S.: Progress in the study and management of river ice jams, Cold Reg. Sci. Technol., 51, 2-19, https://doi.org/10.1016/j.coldregions.2007.09.001, January 2008a.

Beltaos, S.: River Ice Break-up, edited by: Beltaos, S., Water Resources Publications, Chelsea, Michigan, 327–348, 2008b.

Beltaos, S.: Hydrodynamic characteristics and effects of river waves caused by ice jam releases, Cold Reg. Sci. Technol., 85, 42–55, https://doi.org/10.1016/j.coldregions.2012.08.003, 2013.

Beltaos, S.: The Drying Peace–Athabasca Delta, Canada: Review and Synthesis of Cryo-Hydrologic Controls and Projections to Future Climatic Conditions, Sustainability 2023, 15, 2103, https://doi.org/10.3390/su15032103, 1 February 2023.

Beltaos, S. and Prowse, T.: River-ice hydrology in a shrinking cryosphere, Hydrol. Process., 23, 122-144, https://doi.org/10.1002/hyp.7165, 2009.

Beltaos, S., Miller, L., Burrell, B. C., and Sullivan, D.: Formation of Break-up Ice Jams at Bridges, J. Hydraul. Eng. 132(11), https://doi.org/10.1061/(ASCE)0733-9429(2006)132:11(1229), 2006.

Beltaos, S., Tang, P., and Rowsell, R.: Ice jam modelling and field data collection for flood forecasting in the Saint John River, Canada, Hydrol. Process., 26, 2535–2545, https://doi.org/10.1002/hyp.9293, 2012.

Beltaos, S.: Effects of climate on river ice jams, in: The 9th Workshop on River Ice, 24–26, 1997.

Benda, L., Miller, D., and Barquän, J.: Creating a catchment scale perspective for river restoration, Hydrol. Earth Syst. Sci., 15, 2995–3015, https://doi.org/10.5194/hess-15-2995-2011, 2011.

Beven, K. J., Kirkby, M. J., Schofield, N., and Tagg, A. F.: Testing a physically based flood forecasting model (TOPMODEL) for three U.K. catchments, J. Hydrol. 69(1-4), 119–143, https://doi.org/10.1016/0022-1694(84)90159-8, 1984.

Blouin, C., Ghobrial, T., Morse, B., Pelchat, G., and Turcotte, B.: The influence of tributaries on break-up dynamics: Insights from the Chaudière River, Québec, in: 21st Workshop on the Hydraulics of Ice-Covered Rivers, Saskatoon, Saskatchewan, Canada, August 29-September 1, 2021.

Buzin, V. A.: Ice Dams and Dam Floods on Rivers, Gidrometeoizdat, St. Petersburg, 2004.

Campolo, M., Andreussi, P., and Soldati, A.: River flood forecasting with a neural network model, Water Resour. Res., 35, 1191–1197, https://doi.org/10.1029/1998WR900086, 1999.

Cloke, H. L. and Pappenberger, F.: Ensemble flood forecasting: A review, J. Hydrol. 375(3-4), 613-626, https://doi.org/10.1016/j.jhydrol.2009.06.005, 15 September 2009.

Das, A., Rokaya, P., and Lindenschmidt, K.-E.: Assessing the impacts of climate change on ice jams along the Athabasca River at Fort McMurray, 19th Workshop on the Hydraulics of Ice-Covered Rivers, Alberta, Canada, 2017.

De Munck, S., Gauthier, Y., Bernier, M., Chokmani, K., and Légaré, S.: River predisposition to ice jams: A simplified geospatial model, Nat. Hazards Earth Syst. Sci. (17), 1033–1045, https://doi.org/10.5194/nhess-17-1033-2017, 2017.

De Rham, L., Dibike, Y., Beltaos, S., Peters, D., Bonsal, B., and Prowse, T.: A Canadian River Ice Database from the National Hydrometric Program Archives, Earth Syst. Sci. Data, 12, 1835–1860, https://doi.org/10.5194/essd-12-1835-2020, 2020.

Dutton, G.: Scale, Sinuosity and point selection in digital line generalisation, Cartogr. Geogr. Inf. Sci. (26), 33–53, 1999.

French, H. M.: The Periglacial Environment, John Wiley & Sons Ltd, 2018.

Gauthier, Y., Paquet, L.-M., Gonzalez, A., and Bernier, M.: Using radar images and GIS to support ice-related flood forecasting, Geomatica, 62(2), 139–149, 2008.

Insurance Bureau of Canada: https://www.newswire.ca/news-releases/fort-mcmurray-flooding-causes-over-228-million-in-insured-damage-837624948.html, last access: 25 February 2025.

Kalinin, V. G.: Study of spatial distribution and occurrence frequency of ice jams in rivers of the Votkinsk reservoir catchment, Russ. Meteorol. Hydrol., 33, 819–822, https://doi.org/10.3103/S1068373908120091, 2008.

Kawai, T., Hara, F., Masaki, S., Nishihata, A., and Saeki, H.: Experimental Study on the Process of Ice Jam Development, in: The 9th Workshop on River Ice, 245–256, 1997.

Kowshal, A., Das, A., and Lindenschmidt, K. E.: Developing a geospatial model to predict locations of higher propensity to ice jamming along the Saint John River, CGU HS Committee on River Ice Processes and the Environment, 21st Workshop on the Hydraulics of Ice Covered Rivers, Saskatoon, Saskatchewan, Canada, August 29 - September 01, 2021.

Kozlov, D. V. and Kuleshov, S. L.: Multidimensional Data Analysis in the Assessment of Ice-Jam Formation in River Basins, Water Resour., 46, 152–159, https://doi.org/10.1134/S0097807819020088, 2019.

Lex, A., Gehlenborg, N., Strobelt, H., Vuillemot, R., and Pfister, H.: UpSet: Visualisation of intersecting sets, IEEE Trans. Vis. Comput. Graph, 20, 1983–1992, https://doi.org/10.1109/TVCG.2014.2346248, 2014.

Lindenschmidt, K.-E., Sydor, M., Carson, R., and Harrison, R.: Ice Jam Modelling of the Lower Red River, J. Water Resour. Prot., 04, 1–11, https://doi.org/10.4236/jwarp.2012.41001, 2012.

Lindenschmidt, K. E. and Das, A.: A geospatial model to determine patterns of ice cover break-up along the Slave River, Can. J. Civ. Eng., 42, 675–685, https://doi.org/10.1139/cjce-2014-0377, 2015.

Lucie, C., Nowroozpour, A., and Ettema, R.: Ice Jams in Straight and Sinuous Channels: Insights from Small Flumes, J. Cold Reg. Eng., 31, https://doi.org/10.1061/(asce)cr.1943-5495.0000123, 2017.

Madaeni, F., Lhissou, R., Chokmani, K., Raymond, S., and Gauthier, Y.: Ice jam formation, break-up and prediction methods based on hydroclimatic data using artificial intelligence: A review, Cold Reg. Sci. Technol., 174, https://doi.org/10.1016/j.coldregions.2020.103032, 1 June 2020.

Madaeni, F., Chokmani, K., Lhissou, R., Homayouni, S., Gauthier, Y., and Tolszczuk-Leclerc, S.: Convolutional neural network and long short-term memory models for ice-jam predictions, Cryosphere, 16, 1447–1468, https://doi.org/10.5194/tc-16-1447-2022, 2022.

Mahabir, C., Hicks, F., and Fayek, A. R.: Neuro-fuzzy River ice break-up forecasting system, Cold Reg. Sci. Technol., 46, 100–112, https://doi.org/10.1016/j.coldregions.2006.08.009, 2006.

Mahabir, C., Hicks, F. E., and Fayek, A. R.: Transferability of a neuro-fuzzy river ice jam flood forecasting model, Cold Reg. Sci. Technol., 48, 188–201, https://doi.org/10.1016/j.coldregions.2006.12.004, 2007.

Massie, D. D., White, K. D., and Daly, S. F.: Application of neural networks to predict ice jam occurrence, Cold Reg. Sci. Technol., 35, 115–122, 2002.

McPherson, J. M. and Myers, R. A.: How to infer population trends in sparse data: Examples with opportunistic sighting records for great white sharks, Divers. Distrib., 15, 880–890, https://doi.org/10.1111/j.1472-4642.2009.00596.x, 2009.

Ministère de la Sécurité publique du Québec (MSP): Historique (publique) d'embâcles répertoriés au MSP, Données Québec, shapefile dataset, available at: https://www.donneesquebec.ca/recherche/dataset/historique-publique-d-embacles-repertories-au-msp, last access: 2024, 2024.

Ministère des Ressources naturelles et des Forêts (MRNF): Géobase du réseau hydrographique du Québec (GRHQ), Données Québec, shapefile download index, available at: https://www.donneesquebec.ca/recherche/fr/dataset/grhq, last access: 2024, 2024.

Ministère des Transports et de la Mobilité durable du Québec (MTMD): Structure, Données Québec, available at: https://www.donneesquebec.ca/recherche/dataset/structure, last access: 2024, 2024.

https://doi.org/10.5194/egusphere-2026-2457
Preprint. Discussion started: 15 July 2026

Morgan, T., Furman, L., and White, K.: Ice Jams, Winter 2002–2003, ERDC/CRREL Technical Note 04-5, U.S. Army Engineer Research and Development Center, Cold Regions Research and Engineering Laboratory, Hanover, New Hampshire, 2004.

Morgan, T., Furman, L., and White, K.: Ice Jams, Winter 2002–2003, ERDC/CRREL Technical Note 04-5, U.S. Army Engineer Research and Development Centre, Cold Regions Research and Engineering Laboratory, Hanover, New Hampshire, 2004.

Mu, X., Bao, J., and Chen, Y.: Floating ice transport conditions at the cross-sections between pier columns in open ice-water two-phase flow canals, Water (Switzerland), 12, https://doi.org/10.3390/w12061813, 2020.

Neary, L., Remmer, C. R., Owca, T. J., Girard, C. A. M., Kay, M. L., Wiklund, J., Imran, A., Hall, R. I., and Wolfe, B. B.: A framework for integrated monitoring of status and trends in water balance, water chemistry and contamination of shallow lakes across a remote dynamic freshwater delta, EarthArXiv [preprint], https://doi.org/10.31223/x5mh4p, 2023.

Oubennaceur, K., Chokmani, K., Nastev, M., Lhissou, R., and El Alem, A.: Flood risk mapping for direct damage to residential buildings in Quebec, Canada, Int. J. Disaster Risk Reduct., 33, 44–54, https://doi.org/10.1016/j.ijdrr.2018.09.007, 2019.

Rokaya, P., Budhathoki, S., and Lindenschmidt, K. E.: Trends in the Timing and Magnitude of Ice-Jam Floods in Canada, Sci. Rep., 8, https://doi.org/10.1038/s41598-018-24057-z, 2018.

She, Y., Andrishak, R., Hicks, F., Morse, B., Stander, E., Krath, C., Keller, D., Abarca, N., Nolin, S., Tanekou, F. N., and Mahabir, C.: Athabasca River ice jam formation and release events in 2006 and 2007, Cold Reg. Sci. Technol., 55, 249–261, https://doi.org/10.1016/j.coldregions.2008.02.004, 2009.

Smith, D. G. and Pearce, C. M.: Ice jam-caused fluvial gullies and scour holes on northern river flood plains, Geomorphology, 42, 85–95, 2002.

Sun, W.: River ice break-up timing prediction through stacking multi-type model trees, Sci. Total Environ., 644, 1190–1200, https://doi.org/10.1016/j.scitotenv.2018.07.001, 2018.

Taha, W., Carbonneau, A.-S., Larouche, M.-È., Shakibaeinia, A., Billy, C., and Lokhmanets, I.: Physical and Numerical Modelling of Ice Jam Initiation due to River Morphological Features, 26th IAHR International Symposium on Ice, Montréal, Canada, 19-23 June 2022, 2022.

Tymiński, T.: Hydrauliczne badania modelowe filarów mostowych na przykładzie wybranych mostów Opola [Hydraulic Model Research on Bridge Piers Based on the Example of Selected Bridges in Opole, in Polish], Rocznik Ochrona Środowiska (Environmental Protection), 12, 879–893, 2010.

Urroz, G. E., Schaefer, J., and Ettema, R.: Bridge-pier location and ice conveyance in curved channels, J. Cold Reg. Eng., 8, 66–72, 1994.

White, K. D.: Review of prediction methods for break-up ice jams, Can. J. Civ. Eng., 30, 89–100, https://doi.org/10.1139/l02-047, 2003.

White, K. D.: Predicting break-up ice jams using logistic regression, J. Cold Reg. Eng., 10(4), 178–189, https://doi.org/10.1061/(ASCE)0887-381X(1996)10:4(178), 1996.

https://doi.org/10.5194/egusphere-2026-2457
Preprint. Discussion started: 15 July 2026

Yang, X., Pavelsky, T. M., and Allen, G. H.: The past and future of global river ice, Nature, 577, 69–73, https://doi.org/10.1038/s41586-019-1848-1, 2020.

865 Zhao, S.-X., Wang, W.-J., Shi, X.-H., Zhao, S.-N., Wu, Y.-J., Quan, Q., Li, C., Szydlowski, M., Li, W., and Kolerski, T.: Freeze-up ice jam formation in the river bend, a case study on the Inner Mongolia Reach of Yellow River, Crystals (Basel)., 11(6), 631, https://doi.org/10.3390/cryst11060631, 2021.